Flame Spread over Inclined Electrical Wire with Applied AC Electric Fields

Zhisheng Li[1], Ju Han Kim[2], Yu Chun Zhang[1], Jeong Park[3*], Suk Ho Chung[4]

[1] Department of Geosciences and Environmental Engineering, Southwest Jiaotong University, Chengdu, China
[2] Department of Mechanical Engineering, Ulsan National Institute of Science and Technology, Ulsan, Korea
[3] Department of Mechanical Engineering, Pukyong National University, Busan, Korea
[4] King Abdullah University of Science and Technology (KAUST), Clean Combustion Research Center (CCRC), Thuwal, Saudi Arabia

Abstract

Effects of applied electric fields on downward and upward flame spreads (DFS and UFS) over polyethylene (PE) insulated electrical wires with Cu-core are experimentally investigated by varying the applied voltage and frequency at various inclination angles. For the baseline case without applying electric field, the flame width and flame spread rate (FSR, S_w) against θ show U-shaped behaviors having minimum values near $\theta = -10°$. With applying AC electric fields, FSRs are influenced appreciably by complex dynamic behaviors of molten PE and flame. For the DFSs, the FSR with θ exhibits increasing, then decreasing, and again increasing trends, while having linear dependence on $\log(f_{AC})$. For the UFSs, the FSR with θ shows an increasing tendency, along with complex dependencies on V_{AC} and f_{AC}. Dynamic behaviors of molten PE (such as downward flow of molten PE, dielectrophoresis, fuel vapor-jet, and electrospray) play important roles on FSR behaviors. These FSR behaviors for DFS ($\theta = -70°$) and UFS ($\theta = 70°$) with Cu-core are well characterized with their related physical parameters.

1 Introduction

Electrical wire fires can be initiated by unexpected overheating and/or short circuit, resulting in an ignition of neighboring flammable materials and thereby causing potential fire hazards in residential and commercial buildings, power plants, industrial complexes, aircrafts, and spacecrafts. The Swissair flight 111 accident in 1998 was caused by an electrical wire initiated by an arc from wire harness [1]. At least five incidents of electrical short circuits or component overheating have been reported on space shuttle missions [2, 3]. Wire fires have been identified as one of the major risk factors in space exploration mission, since the disaster of Apollo 1. NASA has developed the safety codes for electrical wires used in space [4].

In this regard, fundamental characteristics on ignition and flame spread behaviors have been extensively studied over electrical wires installed horizontally and with inclination angles, considering various factors such as core and insulation materials, core and insulation thicknesses, ambient flow and pressure, and gravity [8−13].

The established safety code for wire fire and previous studies mentioned above did not, however, consider the effect of electric field on wire fires. When a wire fire occurs due to an electrical short or

Correspondence to: jeongpark@pknu.ac.kr

arc, electrical potential can still be applied to the electrical wire even in a situation that electrical circuit is disconnected. When either AC or DC electric field is applied to wires installed horizontally and with inclination angles [14−20], the flame spread rates (FSR) are appreciably modified.

Upward and downward flame spreads over inclined electrical wire can be more complicated by the effects of gravity on molten insulator and buoyancy-induced flow and thereby the balance of heat transfer between a flame and wire. For baseline cases without applying electric field, a U-shaped behavior of FSR was observed with increasing inclination angle [13]. When AC electric fields were applied to inclined polyethylene (PE)-insulated wires with NiCr-core, the size of the flame and its FSR were appreciably influenced [16]. The thermal conductivity of metal core material influenced FSR through the thermal balance mechanism even for baseline cases without applying electric field [13]. Under applied AC electric fields with PE-insulated electrical wire with Cu-core installed horizontally, four different phenomena which had not been found with NiCr-core were observed [19]. However, studies on flame spread over inclined wires with applying AC electric fields with Cu-core have not been studied yet.

The characterization of FSR for PE-insulated electrical wires installed horizontally with applying AC electric fields with NiCr- and Cu-core has been successful with a functional dependence on applied voltage and frequency, area effects of wire and insulation material, and radial gradient of electric field intensity at the outer wire diameter [17, 19]. Such characterization of FSR has not yet been tested for inclined wires under the influence of electric field for NiCr-core [16]. In this regard, the characterization of FSR for inclined wires with Cu-core is important along with NiCr-core for the general applicability.

In the present study, a flame spread over inclined electrical wire with Cu-core is investigated experimentally by varying the applied voltage (V_{AC}) and frequency (f_{AC}) at various inclination angles (θ). For the baseline cases of upward flame spread (UFS) and downward flame spread (DFS) without applying electric field, flame spread rates for inclined electrical wires with Cu−core are measured and compared with those obtained previously with NiCr-core [16]. When AC electric fields are applied to inclined wires with Cu-core, FSRs in UFS and DFS are also compared and discussed at a specified inclination angles of $\theta = \pm 70^{o}$. Special concerns are given to dynamic behaviors of molten PE with Cu-core via comparing those with previous NiCr-core cases. The functional dependence of normalized FSR on applied voltage and frequency, thereby the electric field intensity is explored to test the applicability for inclined wires, which has been successful only for horizontally installed wires with NiCr- and Cu-core [17, 19].

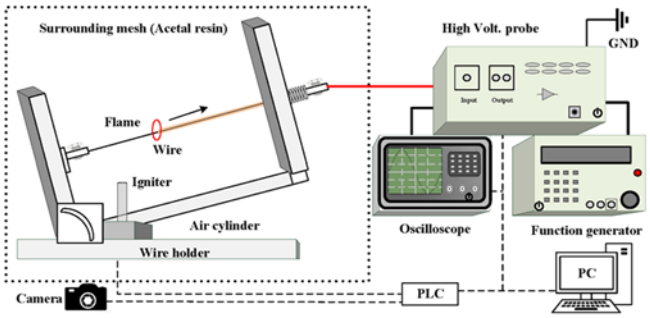

Figure 1: Schematic of experimental setup.

2 Experiment

The apparatus consisted of an electrical wire and wire holder, an AC power supply, and a visualization setup, as schematically shown in Fig. 1. Electrical wires with Cu-core (diameter D_c = 0.5 mm) and polyethylene insulation (with thickness 0.15 mm) were used, yielding the outer diameter (D_{out}) of 0.8 mm. The wire holder was made of non-conductive acetal resin and the test section was surrounded by acetal mesh screens (90×90×90 cm) to prevent outside disturbance.

Details of the experimental procedure have been reported previously [14−20] and are therefore explained briefly. A video camera was triggered to capture images of flame spread, and the recorded images were analyzed using a Matlab-based code. Close-up images were obtained using backlight illumination to visualize the dynamic behaviors of molten PE. High-speed Schlieren images were also taken to distinguish a fuel vapor-jet from fine molten-PE droplets ejected from the surface of molten PE.

An AC power supply (Trek, 10/10B-FG) was used to generate an electric field to the wire. The frequency (f_{AC}) and RMS voltage (V_{AC}) varied in the ranges of 0−1000 Hz and 0−5 kV, respectively, and monitored by using an oscilloscope with a 1000:1 probe (Tektronix, 6015A). The inclination angle of electrical wire varied in the range of −90 to 70°. One end of the wire was connected to the high voltage terminal of the AC power supply and the other end to a building ground.

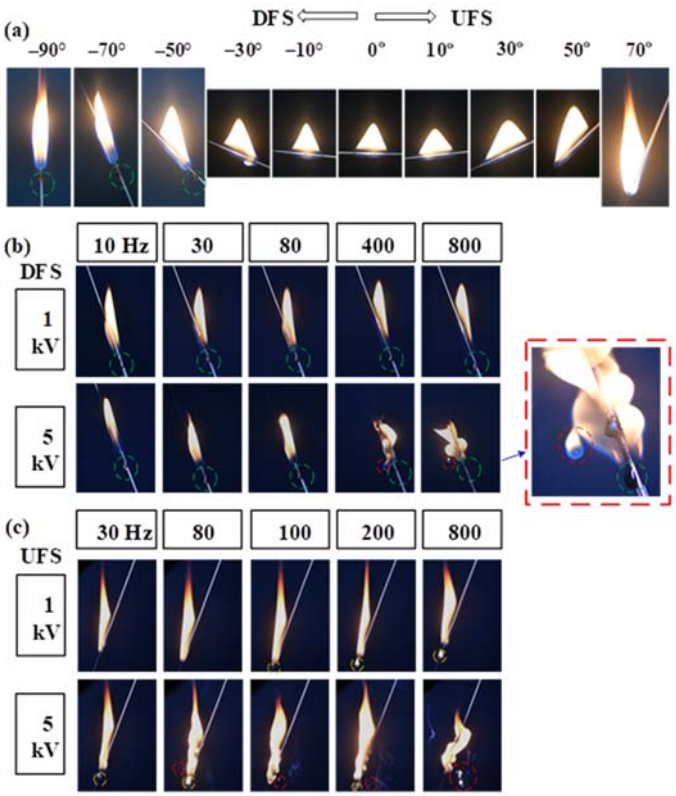

Figure 2: Typical images for downward and upward flame spreads over inclined wire with Cu-core: (a) DFS and UFS against inclination angle for baseline cases with no electric field and (b) DFS ($\theta = -70°$) and (c) UFS ($\theta = 70°$) against frequency at various voltages.

3 Results and discussion

3.1 Overall features of flame spread

Figure 2 shows typical images for the DFSs and UFSs without (a) and with (b,c) applying electric fields. For the baseline case without applying electric field (a), the spreading flame is elongated vertically because of the buoyancy exerted by burnt gas, thus nearly vertical to the wire in the range of $-10° \le \theta \le 10°$. With further decrease (increase) of θ, the DFS (UFS) subsequently leans toward the burnt (unburned) wire side, because the buoyancy effect makes the DFS (UFS) experiencing similar to an opposed (concurrent) flow condition in flame spread [10]. For the UFSs, the flame width increases monotonically with the increase of θ. While for the DFSs, the flame width decreases slightly as θ decreases from 0° to −10°, and then increases with further decrease of θ. As the inclination angle decreases for the DFS, downward flow of molten PE (DFMP) becomes stronger due to the gravity force.

Such molten PE accumulates near the flame front, forming a globular molten PE (GMP) even for the baseline cases in the range of $-90^o \le \theta \le -50^o$, as marked with the green dashed circles, which was also observed previously for DFSs with NiCr-core [16].

An electrophoresis [14−20] leads to soot deposition on the surface of molten PE with electric field, which can be enhanced with increasing voltage. This is exhibited in the enlarged image in Fig. 2b showing the molten PE in black color. Deposited soot particles could enhance radiation absorption to molten PE, reducing surface tension of molten PE. For the DFS with NiCr-core, such downward flow of molten PE leads to a formation of globular molten PE near the flame front [34]. The globular molten PE occasionally drips onto the ground when the size becomes excessively large. However, for the DFS with Cu-core in the present study, a dripping phenomenon of globular molten PE is not observed, while the distance between the flame front and globular molten PE, depending on downward flowrate of molten PE, varies appreciably with frequency and voltage.

For the UFSs (Fig. 2c), the direction of downward flow of molten PE is opposite to that of flame spread. When the applied frequency and/or voltage increases, downward flow of molten PE becomes stronger by the increase in soot deposition on the surface of molten PE. In this situation, several globular molten PEs are sequentially generated. The preceding molten PE continues to flow downward and become far away from the secondary molten PE. Eventually, the flame surrounding the preceding molten PE is detached from the main body of spreading flame. And the third molten PE can be larger than the second one because of evaporation of the second one generated earlier. In such a situation, the third molten PE is merged into the second one quickly. This merged molten PE rotates due to the dielectrophoresis caused by uneven electric field intensity in the circumferential direction of molten PE, such behavior was observed previously for horizontal wire with Cu-core [19].

Deposited soot particles also generate a series of bubbles inside molten PE by heterogeneous nucleation and the bubbles grow due to local heating effects, eventually causing a bubble-bursting phenomenon and then a fuel vapor-jet is ejected from the molten PE surface [15].

When an electric potential is applied to an electrical wire, charges inside the molten PE (either positive or negative) separate and migrate toward the wire or the surface of molten PE (skin layer). When a critical value of applied electric potential is reached, a Taylor cone can be formed. With further increase of electric potential, fine droplets are ejected from the skin layer, resulting in an electrospray phenomenon [16-20]. The difference between electrospray and fuel vapor-jet can be distinguished via taking Schlieren images. When the frequency increases, the occurrence frequency of electrospray increases, forming several small bulged flames. Such small bulged flames point upward due to the effect of buoyancy, heating the unburned wire.

For horizontal electrical wires, uneven electric field intensity between burnt and unburned wires resulted in a dielectrophoresis phenomenon [17−20], where a part of molten PE is detached from the main body of molten PE and subsequently migrates toward the burnt wire side [35]. For the UFSs and DFSs with applied high voltages, multiple globular molten PEs, can be formed inside the flame by dielectrophoretic and downward gravity forces. The directions of these forces are either the same (UFS) or opposite (DFS). A dielectrophoresis phenomenon is not, therefore, clearly observed for UFS at large inclination angles, e.g., $\theta = 70^o$. For DFS with $\theta \ge -50^o$ (although not shown in Fig. 3), migration of molten PE drops toward the burnt wire by dielectrophoresis is observed, which can lead to flame extinction.

3.2 Flame spread Rate

The overall X_f versus t relations are reasonably linear, although not shown here, such that the overall flame spread rate (FSR, S_w) can be defined as $S_w = dX_f/dt$. The FSRs against f_{AC} at various V_{AC} are shown in Fig. 3 at $\theta = \pm 70°$ (a,b), where the dotted line is the baseline case. When AC electric fields are applied to Cu-core with $\theta = -70°$, the FSRs are generally smaller than those of the baseline cases except those for $f_{AC} > 200$ Hz at 1 kV. With $\theta = 70°$ (b), FSRs are generally larger than those of the baseline cases except for certain ranges of f_{AC} for 1 and 2 kV. Note that at $\theta = -70°$ with NiCr-core [34], FSR decreased

with the increases of f_{AC} and V_{AC}. At $\theta = -70°$, FSR behaviors with the Cu-core become quite different from those with the NiCr-core. With the Cu-core, FSR decreases with f_{AC}, e.g., $f_{AC} \leq 80$ Hz at 1 kV, then increases for $80 \leq f_{AC} \leq 600$ Hz, and decreases again for $f_{AC} > 600$ Hz. Similar non-monotonic decreasing and increasing tends are observed at other voltages. For $\theta = 70°$, similar non-monotonic behaviors are observed, while the FSR decreases monotonically with f_{AC} at 1 and 2 kV.

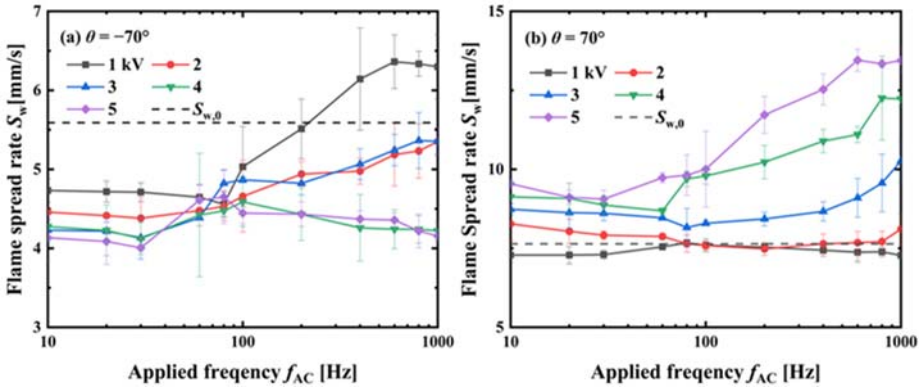

Figure 3: FSR in terms of applied AC electric field and inclination angle; FSR against f_{AC} at various V_{AC} for $\theta = -70°$ (a) and 70° (b).

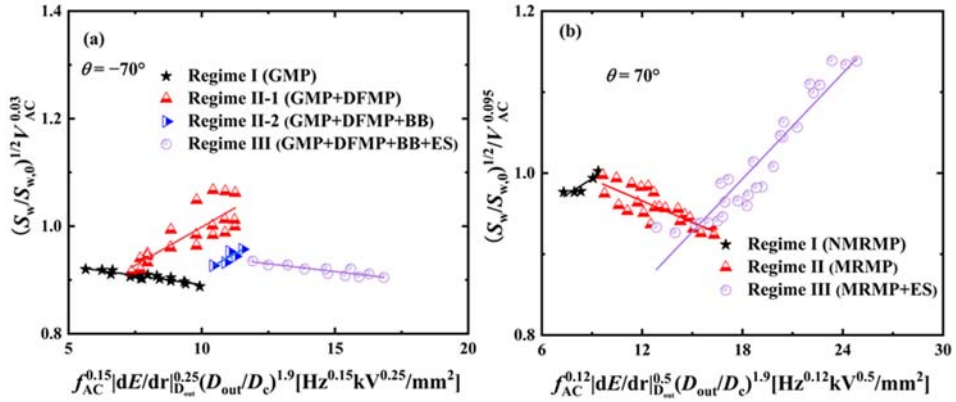

Figure 4: Characterization of flame spread rates for (a) DFS ($\theta = -70°$) and (b) UFS ($\theta = 70°$) with Cu-core.

3.3 Characterization of FSR

For the DFS and UFS with Cu-core, the characterization of FSR is also shown in Fig. 4 with $f = f_{AC}^{0.15} \times |dE/dr|_{D_{out}}^{0.25} \times (D_{out}/D_c)^{1.9}$ [Hz$^{0.15}$×kV$^{0.25}$/mm^2] and $a = 0.03$ for the DFS ($\theta = -70°$) and $f = f_{AC}^{0.12} \times |dE/dr|_{D_{out}}^{0.50} \times (D_{out}/D_c)^{1.9}$ [Hz$^{0.12}$×kV$^{0.5}$/mm^2] and $a = -0.095$ for the UFS ($\theta = 70°$). Satisfactory correlations are also obtained. Because detailed dynamic behaviors of molten PE in each regime were explained in section 3.3, only the best fit results are presented here: (A, B, R) = (−0.069, 0.96, 0.96) in Regime I, (0.028, 0.71, 0.84) in Regime II-1, (0.27, 0.64, 0.88) in Regime II-2, and (−0.0058, 1.0, 0.91) for the DFS, while (0.013, 0.876, 0.90) in Regime I, (−0.0088, 1.071, 0.81) in Regime II, and (0.022, 0.601, 0.95) in Regime III.

4 Conclusions

Effects of applied electric fields on downward and upward flame spreads (DFS and UFS) over polyethylene (PE) insulated electrical wires with Cu-core are experimentally investigated by varying the applied voltage and frequency at various inclination angles.

For the baseline case without applying electric field with Cu-core, the flame width and the flame spread rate against θ had a U-shape behavior having a minimum value at $\theta = -10°$. When

AC electric field is applied with Cu-core, the rates of change of FSR with respect to θ for DFS had increasing (Regime I), decreasing (Regime II), and then increasing (Regime III) tendencies with f_{AC}, which could be characterized with $dS_w/d\theta = a \times \log f_{AC} + b$. Those for UFS showed an increasing tendency, which could be characterized with $dS_w/d\tau = a \times V_{AC}^{2.32} f_{AC}^{0.36} + b$, where $\tau = 1.017^{\theta}$.

Further detailed investigation on the effect of applied AC electric field on FSR was made at $\theta = -70°$ and 70°. Because the characterization of FSR was not made previously with NiCr-core, we here analyzed them and compared with those with Cu-core. With the NiCr-core, FSR behaviors have decreasing tendencies with the increase of frequency for DFS while having decreasing (Regime I) and increasing (Regime II) tendencies for UFS. For the DFS with NiCr-core, such decreasing FSR is associated with the increase in the size of globular molten PE formed near flame front. For UFS with NiCr-core, the decrease in FSR with frequency (Regime I) was related to increase in the occurrence frequency of small flame detachment from the main body of UFS. The increase in FSR with frequency (Regime II) was caused by forcing a series of bulged flames (formed by electrospray phenomenon) to heat the unburned wire. With Cu-core, the FSR behaviors could be grouped into three: decreasing, increasing, and again decreasing tendencies for DFS and increasing, decreasing, and again increasing tendencies for UFS. For the DFS with Cu-core, the decrease in FSR with frequency (Regime I) was caused by the increase of the size of globular molten PE near flame front, which increases the heat capacity of globular molten PE. The increase in FSR (Regime II) was associated with the increase in the distance between globular molten PE and flame front, which reduces heat loss from the spreading flame. The decrease in FSR (Regime III) was related to mass loss of fuel due to electrospray phenomenon. For the UFS with Cu-core, the increase in FSR with frequency (Regime I) was observed because of the increase in flame width due to a downward flow of molten PE. The decrease in FSR (Regime II) was caused by a merging phenomenon between molten PEs flowing inside the flame. The increase in FSR (Regime III) was caused by forcing a series of bulged flames (formed by electrospray phenomenon) to heat the unburned wire. These FSR behaviors in spreading flames over inclined wires with NiCr- and Cu-core can be well characterized with $(S_w/S_{w,0})^{1/2} V_{AC}^{a}\ [\mathrm{kV}^a] = A \times f(f_{AC}, |dE/dr|_{D_{out}}, D_{out}/D_c) + B$. Such behaviors for DFSs and UFSs with Cu-core are also identified in regime diagrams including various dynamic behaviors of molten PE.

Flame extinction was observed only for DFS with NiCr- and Cu-core. For DFS with NiCr-core, flame extinction occurred because of increase of the size of globular molten PE and therefore excessive heat loss from the flame to evaporate globular molten PE. For DFS with Cu-core, the occurrence of vigorous dielectrophoresis phenomenon induced a continuous upward flow toward the burnt wire. When the upward flow dominated over the downward flow by the gravity, a rear part of flame is detached from the main body of DFS, reducing the flame size of DFS. When the flame size of DFS becomes excessively small, the flame is extinguished. Although the extinction mechanisms for DFS with NiCr- and Cu-core are different, the extinction frequency could be characterized with a functional form of $\log f_{AC,ext}\,[\mathrm{Hz}] = A \times V_{AC}\,[\mathrm{kV}] + B$. It was shown that DFSs with NiCr-core are more prone to flame extinction than those with Cu-core.

References

[1] F. Jia, M. Patel, E. Galea, A. Grandison, J. Ewer, CFD fire simulation of the Swissair flight 111 in-flight fire – Part 1: Prediction of the pre-fire air flow within cockpit and surrounding areas, The Aeronautical Journal 110 (2006) 41-52.
[2] R. Friedman, Fire safety in spacecraft, Fire and Materials 20 (1996) 235−243.
[3] T. Limero, S. Wilson, S. Perlot, J. James, The role of environmental health system air quality monitors in space station contingency operations, SAE Technical Paper (1992) 921414.
[4] Flammability, offgassing, and compatibility requirements and test procedures, NASA STD 6001B (2011).
[5] M. Kikuchi, O. Fujita, K. Ito, A. Sato, T. Sakuraya, Experimental study on flame spread over wire insulation in microgravity, Proc. Combust. Inst. 27 (1998) 2507−2514.
[6] O. Fujita, M. Kikuchi, K. Ito, K. Nishizawa, Effective mechanisms to determine flame spread rate over ethylene-tetrafluoroethylene wire insulation: discussion on dilution case effect based on temperature measurements**,** Proc. Combust. Inst. 28 (2000) 2905−2911.
[7] O. Fujita, K. Nishizawa, Effect of low external flow on flame spread over polyethylene-insulated wire in microgravity**,** Proc. Combust. Inst., 29 (2002) 2545−2522.
[8] A. Umemura, M. Uchida, T. Hirata, J. Sato, Physical model analysis of flame spreading along an electrical wire in microgravity, Proc. Combust. Inst., 29 (2002), pp. 2535−2543.
[9] Y. Nakamura, N. Yoshimura, H. Ito, K. Azumaya, O. Fujita, Flame spread over electric wire in sub-atmospheric pressure, Proc. Combust. Inst. 32 (2009) 2559−2566.
[10] L. Hu, Y. Zhang, K. Yoshioka, H. Izumo, O. Fujita, Flame spread over electric wire with high thermal conductivity metal core at different inclinations, Proc. Combust. Inst. 35 (2015) 2607−2614.
[11] L. Hu, Y. Lu, K. Yoshioka, Y. Zhang, C. Fernandez-Pello, S.H. Chung, O. Fujita, Limiting oxygen concentration for extinction of upward spreading flames over inclined thin polyethylene-insulated NiCr electrical wires with opposed-flow under normal- and micro-gravity, Proc. Combust. Inst. 36 (2017) 3045−3053.
[12] Y. Kobayashi, X. Huang, S. Nakaya, M. Mitsuhiro, C. Fernandez-Pello, Flame spread over horizontal and vertical wires: the role of dripping and core, Fire Safety J 91 (2017), 112−122.
[13] X. Huang, Y. Nakamura, A review of fundamental combustion phenomena in wire fires, Fire Technol 56 (2020) 315−360.
[14] M.K. Kim, S.H. Chung, O. Fujita, Effect of AC electric fields on flame spread over electrical wire, Proc. Combust. Inst. 33 (2011) 1145−1151.
[15] S.J. Lim, M.K. Kim, J. Park, O. Fujita, S.H. Chung, Flame spread over electrical wire with AC electric fields: internal circulation, fuel vapor-jet, spread rate acceleration, and molten insulator dripping, Combust. Flame 162 (2015) 1167−1175.
[16] S.J. Lim, S.H. Park, J. Park, O. Fujita, S.I. Keel, S.H. Chung, Flame spread over inclined electrical wires with AC electric fields, Combust. Flame 185 (2017) 82−92.
[17] S.H. Park, S.J. Lim, M.S. Cha, J. Park, S.H. Chung, Effect of AC electric field on flame spread in electrical wire: variation in polyethylene thickness and di-electrophoresis phenomenon, Combust. Flame 202 (2019) 107−118.
[18] M.S. Kang, C.S. Yoo, J. Park, S.H. Chung, Effect of metal core on flame spread over electrical wire with applied electric fields, Proc. Combust. Inst. 38 (2021) 4747−4756.
[19] M.S. Kang, J. Park, S.H. Chung, C.S. Yoo, Effect of the thickness of polyethylene insulation on flame spread over electrical wire with Cu-core under AC electric fields, Combust. Flame (2022) 112017.
[20] S.H. Park, M.S. Kang, M.S. Cha, J. Park, S.H. Chung, Flame spread over twin electrical wires with applied DC electric fields, Proc. Combust. Inst. 210 (2019) 350−359.